Satellite boreal measurements over Alaska and Canada during June–July 2004: Simultaneous measurements of upper tropospheric CO, C_2H_6, HCN, CH_3Cl, CH_4, C_2H_2, CH_3OH, HCOOH, OCS, and SF_6 mixing ratios

Curtis P. Rinsland,[1] Gaëlle Dufour,[2] Chris D. Boone,[3] Peter F. Bernath,[3,4] Linda Chiou,[5] Pierre-François Coheur,[6] Solène Turquety,[7] and Cathy Clerbaux[7]

Received 18 July 2006; revised 21 May 2007; accepted 31 May 2007; published 8 August 2007.

[1] Simultaneous ACE (Atmospheric Chemistry Experiment) upper tropospheric CO, C_2H_6, HCN, CH_3Cl, CH_4, C_2H_2, CH_3OH, HCOOH, and OCS measurements show plumes up to 185 ppbv (10^{-9} per unit volume) for CO, 1.36 ppbv for C_2H_6, 755 pptv (10^{-12} per unit volume) for HCN, 1.12 ppbv for CH_3Cl, 1.82 ppmv (10^{-6} per unit volume) for CH_4, 0.178 ppbv for C_2H_2, 3.89 ppbv for CH_3OH, 0.843 ppbv for HCOOH, and 0.48 ppbv for OCS in western Canada and Alaska at 50°N–68°N latitude between 29 June and 23 July 2004. Enhancement ratios and emission factors for HCOOH, CH_3OH, HCN, C_2H_6, and OCS relative to CO at 250–350 hPa are inferred from measurements of young plumes compared with lower mixing ratios assumed to represent background conditions based on a CO emission factor derived from boreal measurements. Results are generally consistent with the limited data reported for various vegetative types and emission phases measured in extratropical forests including boreal forests. The low correlation between fire product emission mixing ratios and the SF_6 mixing ratio is consistent with no significant SF_6 emissions from the biomass fires.

Citation: Rinsland, C. P., G. Dufour, C. D. Boone, P. F. Bernath, L. Chiou, P.-F. Coheur, S. Turquety, and C. Clerbaux (2007), Satellite boreal measurements over Alaska and Canada during June–July 2004: Simultaneous measurements of upper tropospheric CO, C_2H_6, HCN, CH_3Cl, CH_4, C_2H_2, CH_3OH, HCOOH, OCS, and SF_6 mixing ratios, *Global Biogeochem. Cycles*, *21*, GB3008, doi:10.1029/2006GB002795.

1. Introduction

[2] Observations and models indicate that as the climate warms, the Arctic warms the most and the fastest [*Manabe et al.*, 1992]. Sea ice and snow cover are decreasing there, and changes in Arctic chemistry and the influx of pollution may disrupt this sensitive system [*Arctic Monitoring Assessment Programme*, 2006; *Rinke et al.*, 2004; *Koch and Hansen*, 2005]. Biomass burning is a major source of trace gases and aerosols [e.g., *Crutzen et al.*, 1979; *Seiler and Crutzen*, 1980; *Duncan et al.*, 2003; *Kasischke et al.*, 2005]. Wildfires are an important emission source in boreal regions during summer and are characterized by large spatial, temporal, and year-to-year variability [*Isaev et al.*, 2002; *Giglio et al.*, 2003]. The large-scale impact of boreal emissions on atmospheric chemistry has been highlighted by ground-based [*Rinsland et al.*, 2000; *Zhao et al.*, 2002; *Yurganov et al.*, 2004] and satellite remote sensing [*Edwards et al.*, 2004; *Liu et al.*, 2005; *Turquety et al.*, 2007].

[3] The occurrence and intensity of boreal fires is expected to increase as evidenced by the increased area burned over Canada over the past three decades as temperatures have warmed [*Gillett et al.*, 2004]. It is projected that the area burned over Canada will double by the end of the century [*Flannigan et al.*, 2005] as the length of the fire season increases over boreal regions [*Stocks et al.*, 1998; *Wotton and Flannigan*, 1993].

[4] Summer 2004 was the warmest on record in interior Alaska, where most of that states forest fires occurred. In addition, it was the third driest with a long drought over much of Alaska. The persistence of high pressure aloft over the Alaskan mainland and the lack of vigorous weather systems were probably the most important factors contributing to the drought over the Alaskan interior, which began on 30 of May and continued through the end of August [*Fathauer*, 2004]. Lightning strikes in Alaska and the Canadian Yukon Territory along with dry conditions during

[1] NASA Langley Research Center, Hampton, Virginia, USA.
[2] Laboratoire de Météorologie Dynamique/Institut Pierre-Simon Laplace, Palaiseau, France.
[3] Department of Chemistry, University of Waterloo, Waterloo, Ontario, Canada.
[4] Now at Department of Chemistry, University of York, York, UK.
[5] Science Systems and Applications, Inc., Hampton, Virginia, USA.
[6] Chimie Quantique et Photophysique, Université Libre de Bruxelles, Brussels, Belgium.
[7] Service d'Aéronomie/Institut Pierre-Simon Laplace, Université Pierre et Marie Curie, Paris, France.

0886-6236/07/2006GB002795$12.00

the second half of June triggered fire activity with >2.7 × 10^6 ha burned, the highest on record to date in Alaska [*Damoah et al.*, 2005, 2006].

[5] Elevated atmospheric CO and sulfate aerosol were measured in Alaska and western Canada by the MOPITT (Measurements Of Pollution In The Troposphere) instrument during summer 2004 [*Pfister et al.*, 2005]. A top-down inverse analysis of the CO emissions from the wildfires that burnt during that time period was reported. The analysis starting with an a priori estimate of 13 Tg CO emitted between June and August 2004 and assuming a uniform vertical distribution of the emissions between the surface and 400 hPa yielded a best a posteriori estimate of 30 ± 5 Tg for the fire emissions from those measurements, MODIS (Moderate Resolution Imaging Spectrophotometer) measurements [*Giglio et al.*, 2003], fire counts, and calculations with a chemical transport model.

[6] More recently a CO emission inventory has been constructed for the boreal 2004 time period [*Turquety et al.*, 2007]. That analysis combined daily area burned reports and MODIS fire hot spots with average estimates of fuel consumption and emission factors based on ecosystem type, partitioning emissions between crown and surface fires, and the burning of the ground-layer organic matter. Estimated total emissions were consistent with MOPITT measurements with a significant fraction of those emissions attributed to peat burning (~30%).

[7] Modeling of boreal emissions such as those measured by MOPITT and from aircraft [*de Gouw et al.*, 2006] requires assumptions of the regional distribution of peat and other fuels and accurate prediction of injection height (the altitude of injection from the top of the fire plume into the boundary layer, free troposphere, or upper troposphere) for each scene. Direct penetration of boreal 2004 fire emissions into the lower stratosphere was reported [*Damoah et al.*, 2005, 2006].

[8] Predicted total June–August 2004 CO emissions from the boreal fires [*Pfister et al.*, 2005] were of comparable magnitude to those of the entire continental U.S. for the same time period with implications for air quality on a hemispheric scale including a near violation of U.S. standards for air quality in the Fairbanks area [*Damoah et al.*, 2006]. Transported air masses reached the Houston area one week later with ozone surface monitors across that area indicating the highest levels of any July day during 2001–2005 [*Morris et al.*, 2006]. Measurements of elevated CO at 500 hPa by AIRS (Atmospheric Infrared Sounder) and aerosol transported from the boreal fires to the Houston area were also reported in that study.

[9] Except for the results noted above, North American measurements for the summer 2004 period of intense boreal burning have lacked key chemical constituents. The objective of this paper is to report the analysis of a time series of simultaneous upper tropospheric measurements of molecular species with a range of lifetimes offering the potential for determination of the relative degree of atmospheric processing [*Smyth et al.*, 1999] and 1.02 μm extinction over western Canada and Alaska at 50°N–68°N latitude between 29 June and 23 July 2004. Measurements of young plumes and lower values assumed to represent background conditions are analyzed to infer the first space-based estimates of boreal emission ratios and emission factors relative to CO for 5 species: HCOOH, C_2H_6, HCN, CH_3OH, and OCS.

[10] The time series were derived from solar occultation measurements recorded by the Atmospheric Chemistry Experiment (ACE) [*Bernath et al.*, 2005] at 50°N–68°N latitude between 29 June and 23 July 2004. They are readily measured in high spectral resolution infrared solar spectra because of their strong absorptions in window regions. Biomass burning is among the identified emission sources for all of these constituents.

[11] The species measured simultaneously by ACE include key components of HO_x (OH + HO_2) chemistry. Current global models have a limited capability to reproduce simultaneous measurements in the dry upper troposphere of nonmethane organic compounds (NMOC), volatile organic compounds (VOC), and oxygenated volatile organic compounds (OVOC). OVOCs are a major source of HO_x (OH + HO_2) in the background troposphere [*Singh et al.*, 2001; *Christian et al.*, 2004], and the production of pollutants in the region is a major concern in the assessment and control strategies of present-day and future air quality in addition to playing a central role in tropospheric ozone production [*Folberth et al.*, 2006].

[12] Carbon monoxide (CO) is a byproduct of incomplete combustion of fossil fuels and biomass, and is produced by oxidation of methane (CH_4) and other hydrocarbons. Reaction with OH is the primary removal mechanism for atmospheric CO [*Logan et al.*, 1981]. Ethane (C_2H_6) is emitted from natural gas leakage, coal mining and biomass burning [*Logan et al.*, 1981]. Hydrogen cyanide (HCN) is a tracer of biomass burning [*Rinsland et al.*, 1998; *Li et al.*, 2000; *Zhao et al.*, 2002; *Singh et al.*, 2003]. Methyl chloride (CH_3Cl) sources are believed to be located mostly in tropical and subtropical terrestrial regions with primary emissions from biomass burning, oceans, and the biosphere, though large uncertainties remain in its budget and the possible impact of climate change on distributions [*World Meteorological Organization*, 2006]. Methane (CH_4) is emitted from at least 10 different sources with major anthropogenic sources that include rice cultivation, livestock, landfills, fossil fuel production and consumption, and biomass burning [*Khahil*, 2000; *Fung et al.*, 1991; *Rinsland et al.*, 2006b]. Biomass burning and combustion are the main sources of ethylene (C_2H_2) [*Gupta et al.*, 1998] with oceanic emissions a possible minor source [e.g., *Kanakidou et al.*, 1988]. Biogenic sources are the most abundant emitters of methanol (CH_3OH), an important organic compound often the second most abundant tropospheric hydrocarbon after methane [*Schade and Goldstein*, 2006]; *Jacob et al.* [2005] with biomass burning 6–10% of the methanol budget [*Jacob et al.*, 2005; *Holzinger et al.*, 2005]. Sources of formic acid (HCOOH) include biomass burning, biogenic emissions from vegetation, secondary production from organic precursors, and motor vehicles [*Rinsland et al.*, 2004, 2006a]. Biomass burning is also a source of carbonyl sulfide (OCS) [*Notholt et al.*, 2003]. It has strong absorption near 5 μm [*Rinsland et al.*, 2002].

[13] We compare measurements of the fire product mixing ratios with simultaneous measurements of SF_6. We

included SF_6 because it is long-lived in both the troposphere and stratosphere [*Ko et al.*, 1993] with emissions mainly from insulating electrical equipment releases. To our knowledge no measurements of SF_6 emissions from biomass fires (e.g., as summarized in biomass burning emission inventories [*Andreae and Merlet*, 2001]) have been reported. Assuming emissions of SF_6 from the boreal fires are negligible, the comparison provides a reference to validate the hypothesis of correlated emission and transport from similar injection heights for the fire-impacted measurement scenes.

[14] Our simultaneous measurements provide evidence that biomass burning was the primary emission source during boreal summer 2004, consistent with mid-July 2004 aircraft in situ mass spectrometer plume measurements of elevated CH_3CN (methyl cyanide) [*de Gouw et al.*, 2006], a biomass burning emission product with a lifetime similar to that of HCN [*Singh et al.*, 2003].

[15] We compare ACE measurements with MOPITT CO mixing ratios (which contain ~1 piece of information in the vertical profile at extratropical latitudes [*Deeter et al.*, 2003]), maps of fire counts, and smoke extinction from nadir images for the July 2004 time period from NOAA thermal infrared channels. Enhancement ratios and emission factors relative to CO for 5 species are inferred. The emission factor from our analysis for each constituent is compared with those reported from previous measurements in extratropical forests including the few sets reported for boreal forests.

[16] Although the emissions from 2004 were the highest on record, boreal fires occur every year. Extensive boreal fires and resulting pollution occurred in 1997 [*Goode et al.*, 2000], 1998 [*Kajii et al.*, 2002], 1990 [*Nance et al.*, 1993], and 2003 [*Jaffe et al.*, 2004]. Satellite images from the summer 1998 fires in boreal Siberia and northern Mongolia were combined with an evaluation of the fire type and emission characteristics to estimate releases of gaseous emissions including CO, CH_4, NO_x, and nonmethane hydrocarbons though measurements of those species were not used to validate their analysis results [*Kajii et al.*, 2002]. Summer fires in Siberia during 2003 increased ozone and CO levels in the Pacific Northwest and contributed to a violation of the ozone air quality standard in that region [*Jaffe et al.*, 2004].

2. ACE Measurements

[17] The Atmospheric Chemistry Experiment (ACE) was launched on 12 August 2003 into a 74° inclined orbit at 650 km altitude [*Bernath et al.*, 2005]. The satellite (also known as SCISAT 1) contains 3 instruments with a shared field of view with the primary goal of recording high-resolution atmospheric spectra by taking advantage of the high precision of the solar occultation technique. Measurements are obtained of a bright source (the Sun) over a (long) limb path through the atmosphere [*Brown et al.*, 1992; *Irion et al.*, 2002, Figure 1]. Distance from the ACE satellite for an atmospheric ray with a tangent altitude of 10 km is ~3000 km. The measurement technique yields limited seasonal and latitudinal limited sampling, though near global annual sampling is achieved by ACE (~85°N–85°S latitude).

[18] The primary instrument is an infrared Fourier transform spectrometer (FTS). It records solar spectra below an altitude of 150 km at a spectral resolution of 0.02 cm^{-1} (maximum optical path difference of ±25 cm) with 750 to 4400 cm^{-1} spectral coverage. The instrument is self-calibrating as low Sun solar spectra are divided by exoatmospheric solar spectra from the same occultation to remove solar features by dividing those measurements by an average of exo-atmospheric spectrum from the same occultation. The procedure also removes the instrument response function as a function of wave number and retains the high signal-to-noise of the individual low Sun observations (see *Norton and Rinsland* [1991] for an example of the use of this method). The instrument is an improvement relative to a similar solar occultation instrument, the Atmospheric Trace MOlecule Spectroscopy (ATMOS) FTS that flew 4 times on the U. S. Shuttle. It used a series of 5 filters, providing limited midinfrared spectral coverage for each occultation event [*Norton and Rinsland*, 1991; *Irion et al.*, 2002]. No measurements were obtained by ATMOS FTS in the visible or near infrared.

[19] Full resolution FTS spectra are recorded by ACE in 2 s. Vertical spacing between successive measurements varies from 2 km for high beta angle (angle between the satellite velocity vector and the vector of the Sun) to 6 km for zero beta angle measurements. Typical vertical altitude spacing between successive measurements is 3–4 km. Visible and near infrared measurements are also obtained from imagers with filters at 0.525 and 1.02 μm (both with a bandpass of ~20–30 nm). Transmission profiles for both the 0.525 and 1.02 μm filters were derived from averages of 3 contiguous pixels centered on the coregistered FTS field of view. Measurements at 1.02 μm are less impacted by extinction sources than those at 0.525 μm, where both O_3 and NO_2 are significant absorbers. Primary extinction at 1.02 μm is due to aerosols and Rayleigh scattering of air with water vapor an additional minor source [*SAGE III ATBD Team*, 2002; *Thomason and Taha*, 2003]. Additional measurements are obtained onboard SCISAT 1 by the MAESTRO (Measurement of Aerosol Extinction in the Stratosphere and Troposphere Retrieved by Occultation) UV-visible spectrometer.

[20] Orbital coverage by ACE yields opportunities to study pollution events in the middle and upper troposphere, and we focus here on CO, C_2H_6, HCN, CH_3Cl, CH_4, CH_3OH, HCOOH, C_2H_2, and OCS from northern hemisphere high latitudes (50°N–68°N) recorded during a period of intense burning activity in Alaska and Canada (29 June to 23 July 2004). Previous ACE studies reported the analysis of elevated CO, C_2H_6, HCN, and C_2H_2 from tropical measurements [*Rinsland et al.*, 2005a], the global CO distribution from the January–September 2004 time period [*Clerbaux et al.*, 2005], CH_3OH from aged tropical biomass burning emissions [*Dufour et al.*, 2006], and tropical-southern midlatitude measurements of HCOOH [*Rinsland et al.*, 2006a].

3. Analysis

[21] Routine ACE FTS science measurements began in February 2004. For the present analysis, we rely on

version 2.2 retrievals [*Boone et al.*, 2005] with updated C_2H_6 results for this investigation. Profiles with statistical uncertainties are retrieved for individual molecules from fits to multiple species in preselected microwindows over prespecified altitude ranges. Temperature profiles are retrieved assuming a realistic CO_2 volume mixing ratio profile accounting for its increase as a function of time. Profiles are obtained from fits to measurements in microwindows selected to provide CO_2 lines covering a wide range of sensitivities with respect to temperature and are constrained to yield an atmosphere in hydrostatic equilibrium. Retrievals below 12 km altitude assume temperatures derived by the Canadian Meteorological Centre (CMC) for the location of the observation.

[22] Spectroscopic parameters and absorption cross sections are based on HITRAN 2004 [*Rothman et al.*, 2005]. Microwindows for CO tropospheric retrievals were selected in the 4209–4277 cm^{-1} region with CH_4 lines as the primary interference. The set of 70 windows for CH_4 span 1245–2888 cm^{-1} and provide 5–55 km altitude coverage. Retrievals for HCN used windows from 3277–3358 cm^{-1}, C_2H_6 retrievals relied on a microwindow at 2976–2977 cm^{-1} [*Rinsland et al.*, 1998], and CH_3Cl was retrieved from a microwindow centered at 2966.98 cm^{-1} with a width of 1.35 cm^{-1}, and an altitude range of 9 to 25 km, fitting for O_3, CH_4, and H_2O as interferences. A single microwindow centered at 948.5 cm^{-1} with a width of 7 cm^{-1} was used to retrieve SF_6 between altitudes of 7 and 31 km. Methanol is retrieved between 7 and 35 km using a large spectral window (984.9–998.7 cm^{-1}) [*Dufour et al.*, 2006]. Our analysis for HCOOH is based on the simultaneous fittings of 5 microwindows from altitudes from 5 to 18 km at the equator with a latitude-dependent maximum altitude, to approximate variations of the tropopause height for the latitudes measured by ACE (85°N–85°S). The selected windows account for interferences overlapping the primary absorption feature of HCOOH, the ν_6 band Q branch at 1105 cm^{-1}. Interferences fitted in the simultaneous analysis were HDO, CH_3D, O_3 isotopologue 2 (i.e., $OO^{18}O$), CCl_2F_2, and CHF_2Cl. Microwindow locations and widths were 1105.15 cm^{-1} and 1.40 cm^{-1}; 2657.23 cm^{-1} and 0.55 cm^{-1}; 1158.55 cm^{-1} and 0.28 cm^{-1}; 1103.63 cm^{-1} and 0.30 cm^{-1}; and 1105.95 cm^{-1} and 0.30 cm^{-1}, respectively. Five windows were used in the OCS retrievals with locations between 2038.90 cm^{-1} and 2052.72 cm^{-1} with CO_2 and O_3 fitted as interferences with windows selected to cover altitudes from 7 to 25 km. Systematic errors include uncertainties in the ACE retrieval algorithm, retrieved temperatures, errors in the tangent heights for individual spectra, and errors in the HITRAN 2004 spectroscopic parameters [*Rothman et al.*, 2005]. Measurements of CH_3CN are not reported in this study as altitude profile retrievals for that molecule from infrared solar occultation spectra are limited to above ~12 km altitude owing to interferences [*Kleinböhl et al.*, 2005], and hence it is less useful than HCN for tropospheric remote sounding of infrared biomass burning emissions.

[23] Figure 1 displays ACE version 2.2 boreal upper tropospheric–lower stratospheric HCN, CO, C_2H_6, HCOOH, CH_3Cl, CH_4, OCS, and CH_3OH volume mixing ratio profiles, which were all measured during sunsets. Retrieved profiles are reported on a 1 km altitude grid with corresponding temperatures and pressures. Noisy measurements have been excluded on the basis of their statistical uncertainties. Mixing ratios up to 185 ppbv for CO, 755 pptv (10^{-12} per unit volume) for HCN, 1.36 ppbv for C_2H_6, 1.12 ppbv for CH_3Cl, 1.82 ppmv for CH_4, 3.89 ppbv for CH_3OH, 0.843 ppbv for HCOOH, and OCS mixing ratios as high as 0.48 ppbv were measured in the upper troposphere. Spacing between tangent heights of successively measured spectra is typically 2–3 km for the occultations and altitude range considered here with the altitude resolution of the retrieved profiles limited to ~4 km by the combined effects of the altitude spacing of the measurements and the finite field of view of the ACE-FTS instrument.

[24] We investigated the origin of the emissions by examining other satellite measurements. Figure 2 illustrates other satellite measurements at about the same time. Figure 2 (top) provides a map of mean CO mixing ratio at 850 hPa for boreal latitudes (29 June to 24 July 2004) from MOPITT. The results show that the air masses captured by ACE coincided with regions of elevated CO in Alaska and western Canada. Maps of CO emissions for the same time period and fire locations derived using MODIS satellite observations after correction for cloud cover (Figure 2, middle) show numerous areas with fire emissions over western boreal North America though CO mixing ratios and fire intensity (based on MODIS pixel density) are lower than in the tropical areas analyzed in a previous study [*Rinsland et al.*, 2005a]. Figure 2 (bottom) shows the area of elevated smoke extinction derived from GOES satellite aerosol data for the same time period. The GASP (GOES Aerosol/Smoke Product) is a dimensionless column product that does not differentiate between smoke, dust, or industrial aerosols.

[25] Figure 3 presents upper tropospheric and lower stratospheric volume mixing ratio vs. altitude profiles of HCN, CO, CH_3Cl, CH_4, C_2H_6, OCS, C_2H_2, SF_6, HCOOH, and CH_3OH for occultation ss5099 (latitude 51.92°N, longitude 285.24°, 24 July 2004). Trop indicates the altitude of the tropopause from NCEP (U.S. Center for Environmental Prediction) measurements for the location and time of the measurement. Figure 1 does not show C_2H_2 because the altitude range of the enhancement is very narrow, and SF_6 is included as a reference. The example shows an occultation measured by ACE with a low minimum measurement altitude for many species. The lowest altitude reached by ACE during an occultation is determined by the increase of atmospheric attenuation due to interfering absorptions, clouds, and smoke along the line of sight. Although the wavelength coverage is different, tropospheric penetration statistics from the SAGE (Stratospheric Aerosol and Gas Experiment) II solar occultation spectra obtained from 1985–1990 at 1.02 μm (where molecular extinction is minimal) with 0.5 km vertical × 2.5 km horizontal resolution penetrated to a minimum altitude of 7 km 50% of the time [*Wang*, 1994; *Wang et al.*, 1996]. The SAGE II statistics from a solar occultation instrument with a similar spatial and vertical resolution as ACE show the upper

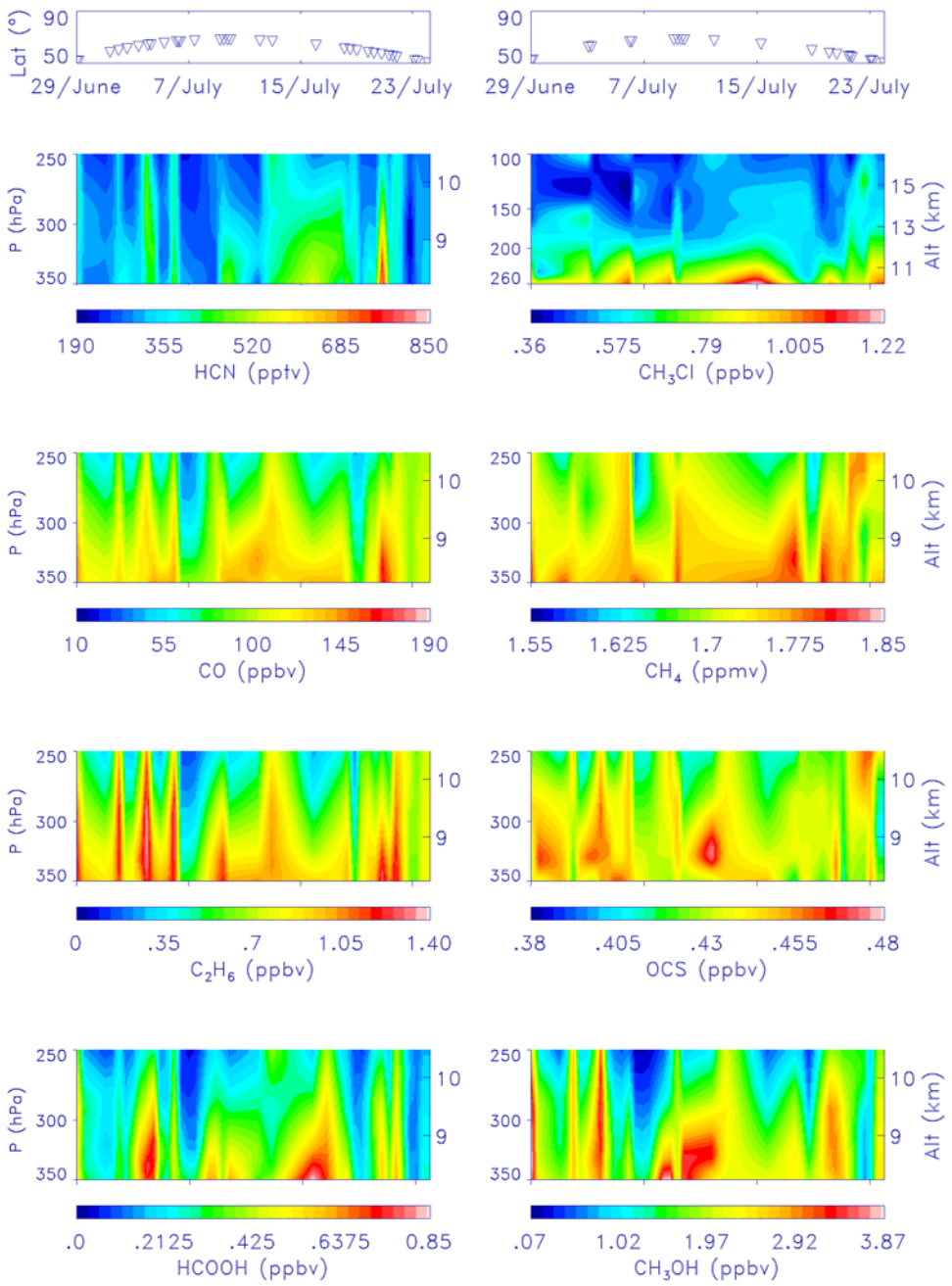

Figure 1. Time series of ACE version 2.2 mixing ratio measurements of HCN, CO, C_2H_6, HCOOH, CH_3Cl, CH_4, OCS, and CH_3OH recorded during sunsets between 29 June and 23 July 2004. The latitude for each observation is shown with inverse triangle above the contours of mixing ratio at 250–350 hPa. Corresponding approximate altitudes are shown on the right vertical axis.

troposphere is often sampled as confirmed by our analysis. Several ACE occultations show elevated mixing ratios extending near the tropopause possibly as a result of deep convection events similar to those reported from Alaska, which induced penetration of gases and particles into the lower stratosphere [*Damoah et al.*, 2005, 2006].

[26] Figure 4 shows plots of the ACE version 2.2 mixing ratios of HCN, C_2H_6, CH_3Cl, CH_4, OCS, HCOOH, CH_3OH, C_2H_2, and SF_6 with corresponding simultaneous measurement of CO mixing ratios. We chose CO as the reference for these comparisons because it has been used as a reference for emission factors from laboratory and atmospheric biomass fire measurements with different fuel types [*Singh et al.*, 2004; *Andreae and Merlet*, 2001; *Paton-Walsh et al.*, 2005; *Koppmann et al.*, 2005]. Correlation coefficients were above 0.6 except for SF_6 ($R^2 = 0.29$) and OCS ($R^2 = 0.41$). As already mentioned, SF_6 is a long-lived tracer in both the troposphere and stratosphere [*Ko et al.*, 1993] with emissions mainly from insulating electrical equipment releases. To our knowledge no measurements

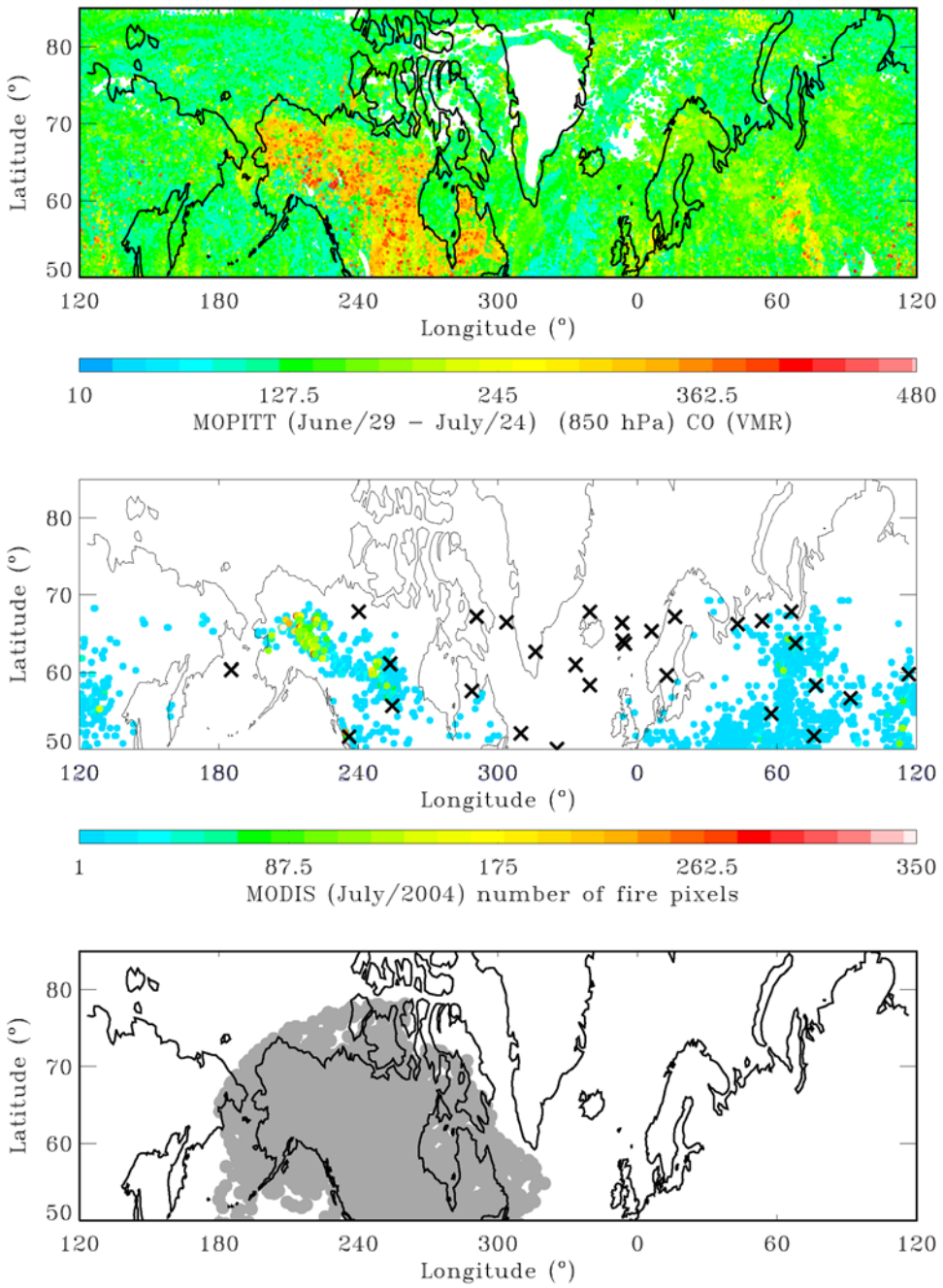

Figure 2. (top) Map of boreal CO mean volume mixing ratio at 850 hPa for July 2004 from MOPITT measurements. (middle) Boreal map at 0.5 km spatial resolution derived from MODIS fire counts for July 2004. Black crosses mark ACE occultation measurement locations. (bottom) Smoke extinction from nadir images for the July 2004 time period from NOAA thermal infrared channels.

of SF_6 emissions from biomass fires have been reported (e.g., as summarized in biomass burning emission inventories [*Andreae and Merlet*, 2001] and in a recent review of biomass burning emissions [*Koppmann et al.*, 2005]).

[27] The low correlation between fire product emission mixing ratios and the SF_6 mixing ratio is consistent with no significant SF_6 emissions from the biomass fires. The higher though limited correlations of upper tropospheric mixing ratios of the individual fire products with those of CO suggest emissions from individual measurements originated from similar injection heights, which likely varied during the measurement time series.

4. Emission Factors

[28] Emission ratios and emission factors were estimated for 5 species relative to CO by comparing mixing ratios measured in plumes with lower values measured during the

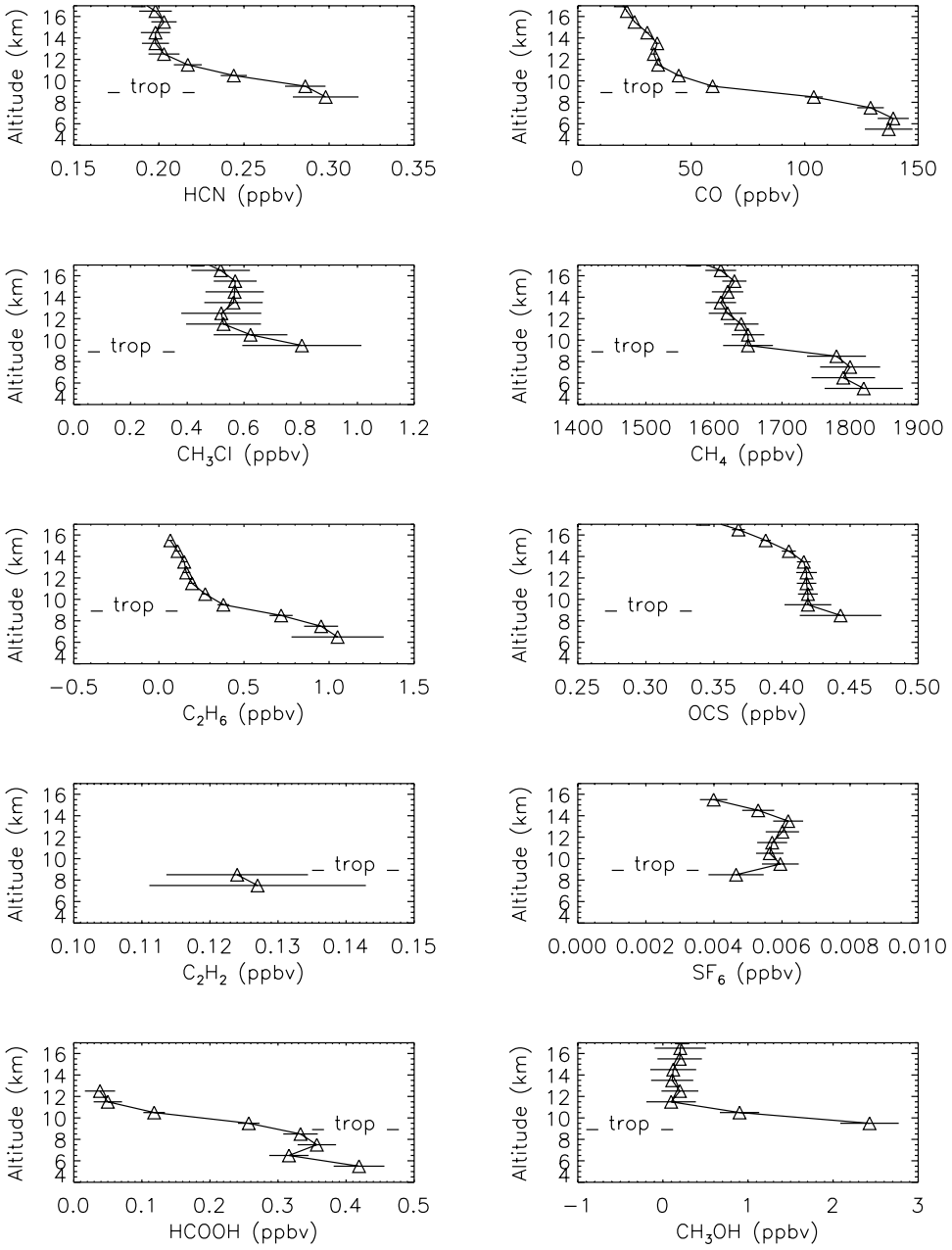

Figure 3. Upper tropospheric and lower stratospheric volume mixing ratio versus altitude profiles of HCN, CO, CH_3Cl, CH_4, C_2H_6, OCS, C_2H_2, SF_6, HCOOH, and CH_3OH from occultation ss5099 (51.92°N, 285.24°). Trop indicates the altitude of the tropopause from NCEP measurements for the location and time of the measurement. Horizontal lines indicate the 1-sigma statistical uncertainty.

ACE measurement time period (29 June and 23 July 2004). As illustrated in Figure 1, measurements covering 250–350 hPa provide good sampling of both elevated and background scenes with about 40 occultations measured by ACE. The conventional, widely used approach was used to determining emission ratios and emission factors. Measured mixing ratios for each species were first plotted versus the corresponding mixing ratio of CO. The slope of the linear relation was used to compute the emission ratio. The ratio (uncertainty/mixing ratio) was used to filter out noisy data. Although both HCN and CH_3CN have been proposed as tracers of biomass fires, neither is a true tracer of fires due the variability of fuel nitrogen in fires [*Christian et al.*, 2004].

[29] The ACE measurement data were converted from emission ratios with respect to CO to emission factors assuming the relation

$$EF_x = ER_{(X/CO)} * (MW_x/MW_{CO}) * EF_{CO}, \quad (1)$$

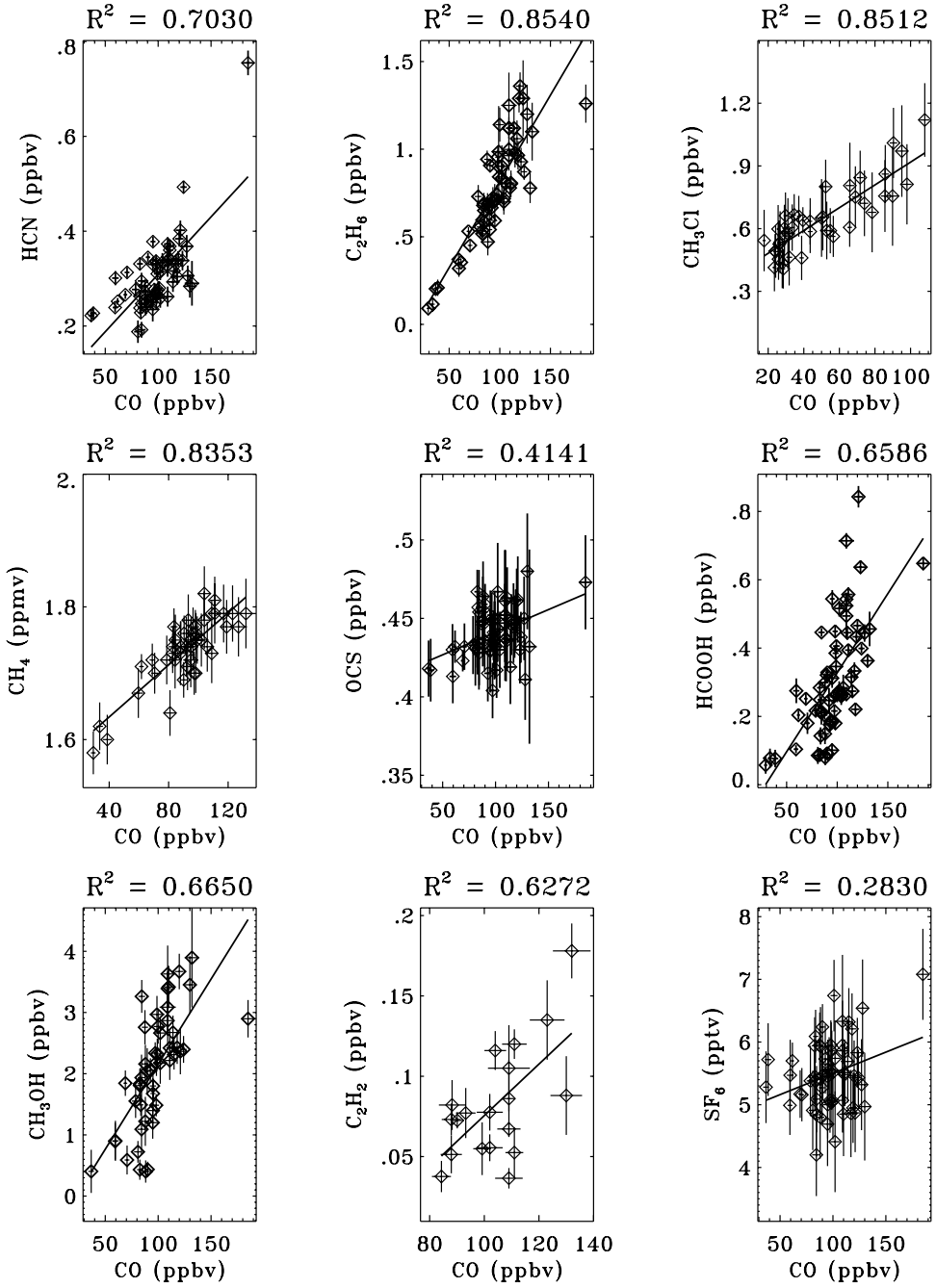

Figure 4. Mixing ratios of HCN, C_2H_6, CH_3Cl, CH_4, OCS, HCOOH, CH_3OH, C_2H_2, and SF_6 mixing ratio correlation with simultaneous mixing ratios measurements of CO at 250 to 350 hPa, except the vertical range is limited to 260 to 100 hPa for CH_3Cl and below 250 hPa for C_2H_2. Error bars indicate standard deviations. Correlation coefficients are reported. Measurements shown are those from the 2004 time period.

where EF_x is the emission factor for the molecular species X, $ER_{(X/CO)}$ is the molar emission ratio of the molecular species with respect to CO, MW_x is the molecular weight of the molecular species, MW_{CO} is the molecular weight of CO, and EF_{CO} is the emission factor for CO [*Andreae and Merlet*, 2001]. We assumed a CO emission factor of 86 ± 17 g kg^{-1} for CO for dry matter. The mean is an average of the emission factors of 81 ± 12 g kg^{-1} determined from airborne measurements from an Alaskan wildfire in an old spruce forest [*Nance et al.*, 1993, Table 2] and 89 g kg^{-1} inferred from airborne Alaskan wildfire airborne measurements [*Goode et al.*, 2000, Table 7]. It is lower than the emission factor of 107 ± 37 g kg^{-1} estimated for dry matter combusted in extratropical forests [*Andreae and Merlet*,

Table 1. Enhancement Ratio Relative to CO and Emission Factor Dry Matter Burned From the ACE Arctic Summer 2004 Time Series and Comparisons With Aircraft and Laboratory Boreal Emission Factor Measurements[a]

Molecule	Emission Ratio Relative to CO	Emission Factor, g kg^{-1}	NF_{ace}	EF(Goode), g kg^{-1}	EF_{RSC}, g kg^{-1}
HCOOH	0.00463 ± 0.00067	0.65384 ± 0.16111	65	0.99	0.34
CH_3OH	0.0278 ± 0.00456	2.73264 ± 0.7065	49	1.66	1.07
HCN	0.00242 ± 0.00032	0.20087 ± 0.05706	62	0.69	0.92
C_2H_6	0.00984 ± 0.00077	0.90645 ± 0.19459	63	0.66	2.71
OCS	0.00029 ± 0.00008	0.05312 ± 0.01844	62		

[a]Derived from 50.2°N–67.8°N latitude measurements between 29 June and 23 July 2004. See text for additional details. NF_{ace} is the number of measurements used to compute the emission ratios and emission factors. Uncertainty for ACE measurements is the 1-sigma standard deviation for each gas. EF(Goode) is the boreal emission factor from airborne measurements [*Goode et al.*, 2000], and EF_{RSC} is the emission factor derived for residual smoldering combustion of boreal fuels from laboratory fire measurements [*Bertschi et al.*, 2003, Table 3].

2001, Table 1]. Our selected emission factor is likely to be more appropriate for the boreal region sampled by the ACE measurements. Emission factors for CO from helicopter sampling measurements in the Canadian Northwest Territories [*Cofer et al.*, 1998, Table 2] were limited to sampling of high-intensity crown fires.

[30] A large variety of trace gases are emitted during the smoldering stage of fires, and therefore the emission of most of them is strongly correlated with that of CO [*Koppmann et al.*, 2005], although a CO emission factor range of at least a factor of two has been reported [*Koppmann et al.*, 2005], consistent with the wide range of CO emissions from smoldering fires measured in a laboratory open combustion facility [*Yokelson et al.*, 1997, Table 1]. Other species have been used as a reference to calculate emission ratios and emission factors. In particular, CO_2 has been employed as a reference for flaming products [*Shirai et al.*, 2003]. The potential for bias in adopting CO as a reference has been noted [e.g., *Andreae and Merlet*, 2001].

[31] Table 1 reports the enhancement ratios relative to CO and the corresponding emission factor from the ACE 2004 boreal data obtained from the background and plume occultations. Uncertainties reported in this table are statistical uncertainties calculated from the version 2.2 profiles, which are reported on a vertical grid with 1 km vertical spacing in altitude. We include for comparison boreal emission factors derived from airborne measurements [*Goode et al.*, 2000] and from laboratory measurements of residual smoldering combustion from large diameter and belowground biomass fuels [*Bertschi et al.*, 2003].

[32] The 5 species selected for determination of enhancement ratios and emission factors are minimally impacted by photochemistry. Results are inferred from measurements of young plumes, modified by initial chemistry and lofted by convection from the injection altitude to the free troposphere. Species primarily produced through photochemistry such as O_3, are not reported. Although the ACE version 2.2 products include CH_4, inconsistencies in modeling the absorption in the windows in the two primary sampled bands prevented determination of precise and reliable enhancement ratios and emission factors. Tests of the ACE retrievals with a revised set of windows and modified air-broadening coefficients for selected windows in one of the two bands led to improved fits to CH_4 lines in the ACE spectra. If these problems can be resolved, satellite measurements offer the potential for quantifying CH_4 emission ratios and emission factors. A range of 1 to 20 g kg^{-1} in the CH_4 emission factor was reported in a recent review of gaseous emissions from biomass fires [*Koppmann et al.*, 2005, section 5.2]. Short-lived species measured in young plumes by ACE include PAN (peroxyacetyl nitrate CH_3COO_2NO), C_2H_4, H_2CO [*Coheur et al.*, 2007], and H_2O_2 [*Rinsland et al.*, 2007].

[33] Absolute uncertainties of the enhancement ratios and emission factors are difficult to quantify in addition to the potential for error in the assumed CO emission factor as a reference already noted. A fundamental assumption in the ACE retrievals is the vertical profile for CO_2 based on current level and increase rate for CO_2 in the atmosphere. However, it is well established that excess CO_2 is emitted from fires with a typical excess of 5% in extratropical forests [*Yokelson et al.*, 1999; *Hurst et al.*, 1994]. We assume this value as an upper limit for a bias as it was likely reduced by dilution in transport of the fire emissions from the ejection altitude to the upper tropospheric altitudes sampled by ACE. This bias is a source of additional systematic error. Systematic differences in mixing ratios due to differences in the retrieval algorithm are estimated to be 5% or less on the basis of comparisons of ACE profiles with those retrieved for the same scenes with an independently developed algorithm [*Rinsland et al.*, 2005b]. Combining the upper limit for bias due to the assumption of a background CO_2 profile with the upper limits of 5% for algorithm bias suggest ~8% as the bias upper limit, excluding molecule-by-molecule impact of spectroscopic biases in the microwindows used for the version 2.2 analysis with the HITRAN 2004 spectroscopic parameters [*Rothman et al.*, 2005]. A 20% relative uncertainty in the boreal emission factor is assumed, although the emission factors of the two reported boreal measurements agree to <10% [*Nance et al.*, 1993, Table 2; *Goode et al.*, 2000, Table 7].

[34] Additional systematic errors are errors in the molecular spectroscopy assumed in the retrievals, which depend on the molecular species and possible bias in the assumed emission factor for CO. The main source of spectroscopic error is possible bias in the absolute intensity of the target absorption features. Those errors are 5–10% with the possible exception of HCOOH because the sample pressure used in determining the intensities may be in error by as

much as a factor of two due to dimer formation in the laboratory spectra [*Vander Awera and Didriche*, 2004].

[35] We next report molecule-by-molecule comparisons of the ACE emission factors with those from previous studies. We select as a primary reference the emission values reported for extratropical forests from airborne measurements of Alaskan boreal fires [*Andreae and Merlet*, 2001, Table 1]. Differences highlight the uncertainties that remain and the need for additional measurements and investigations, particularly for boreal forests.

4.1. Formic Acid (HCOOH)

[36] The ACE HCOOH emission factor of 0.65 ± 0.16 g kg^{-1} can be compared with the wide range of emission factors reported from extratropical forests obtained by infrared Fourier transform spectroscopy [*Yokelson et al.*, 1999; *Goode et al.*, 2000; *Paton-Walsh et al.*, 2005]. An emission factor of 1.17 g kg^{-1} was reported from 12 airborne samples from a prescribed fire in North Carolina [*Yokelson et al.*, 1999, Table 2], an emission factor of 0.99 g kg^{-1} was reported from airborne in situ sampling measurements of 4 isolated plumes in the Alaskan boreal forest [*Goode et al.*, 2000, Table 7], and 3.7 ± 2.1 g kg^{-1} derived from Australian temperate forest fire emissions [*Paton-Walsh et al.*, 2005]. An updated emission factor of 2.4 ± 2.3 g kg^{-1} for extratropical forests was cited as an update (M. O. Andreae, personal communication, 2005) by *Paton-Walsh et al.* [2005]. The ACE-inferred emission ratio relative to CO of 0.00463 ± 0.00067 (1 sigma) is close to the boreal fire HCOOH/CO ratio of 0.0062 derived from 1997 boreal fires [*Goode et al.*, 2000, Table 7]. The emission factor of 0.34 g kg^{-1} derived from laboratory measurements of boreal fuels [*Bertschi et al.*, 2003] is lower than the ACE measurement.

4.2. Methanol (CH_3OH)

[37] The emission factor of 2.73 ± 0.71 g kg^{-1} inferred from the ACE measurements is higher than the 2.0 ± 1.40 g kg^{-1} extratropical forest emission factor [*Andreae and Merlet*, 2001, Table 1], the value of 1.35 g kg^{-1} inferred from analysis of Alaska biomass burning plumes [*Goode et al.*, 2000, Table 7], and 2.03 g kg^{-1} measured in a large, isolated North Carolina, U.S.A. plume [*Yokelson et al.*, 1999, Table 2]. It is also higher than the average emission factor of 1.71 g kg^{-1} by averaging 13 measurements obtained with a wide range of techniques [*Yokelson et al.*, 1999, Table 3]. Reactions on the surface of cloud droplets may explain some measured chemical changes in a smoky cloud [*Yokelson et al.*, 2003] whereas secondary production has been invoked to account for unusually high measured CH_3OH enhancements [*Holzinger et al.*, 2005]. The small relative uncertainty of 16% in the ACE CH_3OH enhancement ratio relative to CO of 0.02780 ± 0.00456 from 49 measurements suggests relatively small variations in CH_3OH/CO, and therefore and no obvious evidence for chemical processing of methanol. The low variability is consistent with the conclusion that CH_3OH secondary production in plumes (primarily from methane oxidation) is not likely to be significant [*de Gouw et al.*, 2006; *Lewis et al.*, 2005]. The ACE-measured CH_3OH/CO mean enhancement ratio is consistent with the wide range of previous forest wildfire plume measurements of aged plumes encountered during from 8 aircraft flights over Eastern Canada and New England during July 2004 [*de Gouw et al.*, 2006, Table 3], which includes the time period of the ACE boreal measurements, and CH_3OH/CO enhancement ratios measured by a wide range of techniques [*Goode et al.*, 2000, Table 5] including those over Alaska in June 1999 obtained by airborne Fourier transform spectroscopy [*Goode et al.*, 2000, Table 4]. As discussed by *de Gouw et al.* [2006], the high variability of the CH_3OH/CO ratio from some previous studies suggest that other processes beyond the burning conditions (burning vs. smoldering) such as removal by precipitation or secondary production sometimes affect the CH_3OH/CO enhancement ratio. The emission factor of 1.07 g kg^{-1} derived from laboratory measurements of boreal fuels [*Bertschi et al.*, 2003, Table 3] is lower than the ACE measurement.

4.3. Hydrogen Cyanide (HCN)

[38] The ACE emission factor of 0.20 ± 0.06 g kg^{-1} is higher than 0.15 g kg^{-1} estimated for extratropical forests [*Andreae and Merlet*, 2001, Table 1], but lower than the emission factor measurement of 0.43 ± 0.22 g kg^{-1} inferred from solar absorption measurements through fires at Wollongong, Australia [*Paton-Walsh et al.*, 2005]. Emissions occur primarily during the smoldering phase of combustion [*Rinsland et al.*, 1998], though initial emissions of HCN from fires are well established from observations [*Paton-Walsh et al.*, 2005; *Yokelson et al.*, 2003]. As mentioned earlier, emissions of HCN are highly dependent on fuel nitrogen content [*Yokelson et al.*, 1999; *Goode et al.*, 2000]. As HCN is a well-established fire emission indicator, the ACE time series of simultaneous HCN and CO measurements provide a unique satellite-based set for evaluating the downwind impact of both emissions from the 2004 boreal fires. ACE measurements are the most extensive set of HCN/CO in boreal fires. The emission factor of 0.92 g kg^{-1} derived from laboratory measurements of boreal fuels [*Bertschi et al.*, 2003, Table 3] is a factor of five higher than the ACE measurement.

4.4. Ethane (C_2H_6)

[39] The ACE boreal emission factor of 0.91 ± 0.19 g kg^{-1} and the emission ratio of C_2H_6 relative to CO (0.0098 ± 0.00077) are both higher than the emission factor of 0.66 ± 0.35 g kg^{-1} and the C_2H_6/CO emission ratio of 0.0066 ± 0.0035 inferred from airborne grab sample measurements of a wildfire that burned in an old black spruce tree forest in Alaska during summer of 1990 [*Nance et al.*, 1993, Table 2], though the difference is within the uncertainties. Our more extensive boreal remote sensing measurement set is consistent with those results obtained with a different measurement technique. The ACE C_2H_6 emission factor is much higher than the emission factor of 0.26 ± 0.11 g kg^{-1} inferred from infrared ground-based solar spectra recorded during intense fires near Wollongong, Australia [*Paton-Walsh et al.*, 2005], but consistent with the updated emission factor of 0.73 ± 0.41 g kg^{-1} for extratropical forests cited by *Paton-Walsh et al.*, 2005] as an updated 2005

communication from *Andreae and Merlet* [2001, Table 1]. The ACE mean C_2H_6/CO emission ratio is also lower than 0.048 ± 0.18 reported from 9 Australian tropical savannah fire smoke plume sampling aircraft measurements [*Hurst et al.*, 1994, Table 6]. The emission factor of 2.71 g kg^{-1} derived from laboratory measurements of boreal fuels [*Bertschi et al.*, 2003] is a factor of three higher than the ACE measurement.

4.5. Carbonyl Sulfide (OCS)

[40] The emission factor of 0.053 ± 0.018 g kg^{-1} inferred from the ACE Arctic fire measurements is higher than the range of 0.030–0.036 g kg^{-1} for extratropical forests [*Andreae and Merlet*, 2001, Table 1]. However, the ACE OCS/CO emission ratio of 0.00029 ± 0.00008 is much lower than the OCS/CO emission ratio of 0.04 reported from the analysis of smoldering combustion emissions from fires measured from burning of grass and hardwood fuels in an open combustion facility in Montana, U.S.A. [*Yokelson et al.*, 1997, Table 3].

5. Summary and Conclusions

[41] ACE solar occultation measurements at 50°N–68°N latitude obtained in the upper troposphere between 29 June and 23 July 2004 show volume mixing ratios of CO up to 185 ppbv, HCN mixing ratios as high as 755 pptv, maximum C_2H_6 mixing ratios of 1.36 ppbv, highest mixing ratios of 1.12 ppbv for CH_3Cl, peak CH_4 mixing ratio of 1.82 ppmv, maximum CH_3OH mixing ratio of 3.89 ppbv, a peak HCOOH mixing ratio of 0.843 ppbv, and a maximum OCS mixing ratio of 0.48 ppbv in the upper free troposphere. All species are well-established biomass burning emission products. Emission factors derived for 5 species add to the limited sets previous reported for the boreal region. Emission factors inferred from the ACE measurements are to our knowledge, the first determined from space-based measurements. Random and systematic sources of error have been estimated. The results are generally consistent with the limited previously reported boreal measurements with no evidence for a systematic bias between the ACE and previously reported measurements.

[42] As the Arctic is a key region for climate change undergoing rapid warming, measurements such as the high-precision ACE vertical profiles, those from other satellites with denser measurement coverage, aircraft, and in situ sensors are needed to enable synoptic-scale tracking of pollution and to provide a means to measure the seasonal buildup of Arctic pollution during winter and early spring when heavy polluted loadings from anthropogenic emission sources cause Arctic haze, potentially changing the radiation balance in that region and providing a source for contamination of Arctic ecosystems. More frequent measurements are also needed to track and quantify the chemical composition of pollution plumes. Such plumes often originate from northern midlatitude continents with the large uncertainties regarding the relative contributions from different source regions to Arctic pollution and their role in the production of tropospheric ozone and its precursors. Measurements combined with improved models of injection from source region to higher altitudes can be used to clarify contribution of boreal fire emissions relative to transport of anthropogenic emissions from different lower latitude source regions. The amount of gaseous and particulate carbon released from forest fires is one of the major uncertainties in understanding and closing the global carbon budget and cycle [*Tans et al.*, 1996; *French et al.*, 2004].

[43] ACE CH_3Cl version 2.2 measurements are limited to a minimum altitude of 9 km because of strong absorption by interferences, but they provide the only space-based global tropospheric profile measurements of that molecule. ACE measurements may help in resolving inconsistencies between measured and modeled distributions [*Yoshida et al.*, 2004].

[44] **Acknowledgments.** NASA Langley Research Center was supported by NASA's Upper Atmosphere Research Program and the Atmospheric Chemistry, Modeling, and Analysis Program (ACMAP). Funding for ACE is provided by the Canadian Space Agency and the Natural Sciences and Engineering Research (NSERC) of Canada. Support at Waterloo was also provided by the NSERC-Bomem-CSA-MSC Industrial Research Chair in Fourier Transform Spectroscopy. We acknowledge the National Center for Atmospheric Research for providing the MOPITT Level 3 data. We also thank Shobha Kondragunta and Ana Prados from NOAA for help in understanding the GASP data product displayed in Figure 2. The research in Belgium was funded by the Fonds National de la Recherche Scientifique (FNRS, Belgium), the Belgian Science Policy, and the European Space Agency (ESA-Prodex arrangement C90-219). Financial support by the "Actions de Recherche Concertées" (Communauté Française de Belgique) is also acknowledged.

References

Andreae, M. O., and P. Merlet (2001), Emission of trace gases and aerosols from biomass burning, *Global Biogeochem. Cycles*, *15*, 955–966.

Arctic Monitoring and Assessment Programme (2006), Arctic Monitoring and Assessment Programme (AMAP) Assessment 2006: Acidifying pollutants, arctic haze, and acidification in the Arctic, report, 112 pp., Oslo, Norway. (Available at http://www.grida.no/amap)

Bernath, P. F., et al. (2005), Atmospheric Chemistry Experiment (ACE): Mission overview, *Geophys. Res. Lett.*, *32*, L15S01, doi:10.1029/2005GL022386.

Bertschi, I., R. J. Yokelson, D. E. Ward, R. E. Babbitt, R. A. Susott, J. G. Goode, and W. M. Hao (2003), Trace gas and particle emissions from fires in large diameter and belowground biomass fuels, *J. Geophys. Res.*, *108*(D13), 8472, doi:10.1029/2002JD002100.

Boone, C. D., R. Nassar, K. A. Walker, Y. Rochon, S. D. McLeod, C. P. Rinsland, and P. F. Bernath (2005), Retrievals for the atmospheric chemistry experiment Fourier transform spectrometer, *Appl. Opt.*, *44*, 7218–7231.

Brown, L. R., C. B. Farmer, C. P. Rinsland, and R. Zander (1992), Remote sensing of the atmosphere by high resolution infrared absorption spectroscopy, in *Spectroscopy of the Earth's Atmosphere and the Interstellar Medium*, edited by K. Narahari Rao and A. Weber, Academic Press, San Diego, Calif.

Christian, T. J., B. Kleiss, R. J. Yokelson, R. Holzinger, P. J. Crutzen, W. M. Hao, B. H. Saharjo, and D. E. Ward (2003), Comprehensive laboratory measurements of biomass-burning emissions: 1. Emissions from Indonesian, African, and other fuels, *J. Geophys. Res.*, *108*(D23), 4719, doi:10.1029/2003JD003704.

Christian, T. J., B. Kleiss, R. J. Yokelson, R. Holzinger, P. J. Crutzen, W. M. Hao, T. Shirai, and D. R. Blake (2004), Comprehensive laboratory measurements of biomass-burning emissions: 2. First intercomparison of open-path FTIR, PTIR-MS, and GC-MS/FID/ECD, *J. Geophys. Res.*, *109*, D02311, doi:10.1029/2003JD003874.

Clerbaux, C., P.-F. Coheur, D. Hurtmans, B. Barret, M. Carleer, R. Colin, K. Semeniuk, J. C. McConnell, C. Boone, and P. Bernath (2005), Carbon monoxide distribution from the ACE-FTS solar occultation measurements, *Geophys. Res. Lett.*, *32*, L16S01, doi:10.1029/2005GL022394.

Cofer, C. R., III, E. L. Winstead, B. J. Stocks, J. G. Goldammer, and D. R. Cahoon (1998), Crown fire emissions of CO_2, CO, H_2, CH_4, and TNMHC from a dense jack pine boreal forest fire, *Geophys. Res. Lett.*, *25*, 3919–3922.

Coheur, P., et al. (2007), ACE-FTS observation of a young biomass burning plume: First reported measurements of C_2H_4, C_3H_6O, H_2CO, and PAN by infrared occultation from space, *Atmos. Chem. Phys. Discuss.*, *7*, 7907–7932.

Crutzen, P. J., L. Heidt, J. P. Krasnec, W. H. Pollock, and W. Seiler (1979), Biomass burning as a source of atmospheric gases CO, H_2, N_2O, NO, CH_3Cl, and COS, *Nature*, *282*, 253–256.

Damoah, R., N. Spichtinger, R. Servranckx, M. Fromm, E. W. Eloranta, I. A. Razenkov, P. James, M. Shulski, C. Forster, and A. Stohl (2005), Transport modeling of a pyro-convective event in Alaska, *Atmos. Chem. Phys. Discuss.*, *5*, 6185–6214.

Damoah, R., N. Spichtinger, R. Servranckx, M. Fromm, E. W. Eloranta, I. A. Razenkov, P. James, P. Shulski, C. Forster, and A. Stohl (2006), A case study of pyro-convection using transport model and remote sensing data, *Atmos. Chem. Phys.*, *6*, 173–185.

Deeter, M. N., et al. (2003), Operational carbon monoxide retrieval algorithm and selected results for the MOPITT instrument, *J. Geophys. Res.*, *108*(D14), 4399, doi:10.1029/2002JD003186.

de Gouw, J. A., et al. (2006), Volatile organic compounds composition of merged and aged forest fire plumes from Alaska and western Canada, *J. Geophys. Res.*, *111*, D10303, doi:10.1029/2005JD006175.

Dufour, G., C. D. Boone, C. P. Rinsland, and P. F. Bernath (2006), First space-borne measurements of methanol inside aged tropical biomass burning plumes using the ACE-FTS, *Atmos. Chem. Phys. Dicuss.*, *6*, 3945–3963.

Duncan, B. N., R. V. Martin, A. C. Staudt, R. Yevich, and J. A. Logan (2003), Interannual and seasonal variability of biomass burning emissions constrained by satellite observations, *J. Geophys. Res.*, *108*(D2), 4100, doi:10.1029/2002JD002378.

Edwards, D. P., et al. (2004), Observations of carbon monoxide and aerosols from the Terra satellite: Northern Hemisphere variability, *J. Geophys. Res.*, *109*, D24202, doi:10.1029/2004JD004727.

Fathauer, T. (2004), Fire weather and synoptic conditions during the boundary fire, paper presented at Boundary Fire Workshop, Geophys. Inst., Fairbanks, Alaska.

Flannigan, M. D., K. A. Logan, B. D. Amiro, W. R. Skinner, and B. J. Stocks (2005), Future area burned in Canada, *Clim. Change*, *72*, 1–16, doi:10.1007/s10584-005-5935-y.

Folberth, G. A., D. A. Hauglustaine, J. Lathière, and F. Brocheton (2006), Interactive chemistry in the laboratoire dététorology dynamique general circulation model: Model description and impact analysis of biogenic hydrocarbons on tropospheric chemistry, *Atmos. Chem. Phys.*, *6*, 2273–2319.

French, N. H. F., P. Goovaerts, and E. S. Kasischke (2004), Uncertainty in estimating carbon emissions from boreal forest fires, *J. Geophys. Res.*, *109*, D14S08, doi:10.1029/2003JD003635.

Fung, I., J. John, J. Lerner, E. Matthews, M. Prather, L. P. Steele, and P. J. Fraser (1991), Three-dimensional model synthesis of the global methane cycle, *J. Geophys. Res.*, *96*, 13,033–13,065.

Giglio, L., J. Descloitres, C. O. Justice, and Y. J. Koufman (2003), An enhanced contextual fire detection algorithm from MODIS, *Remote Sens. Environ.*, *87*, 272–283.

Gillett, N. P., A. J. Weaver, F. W. Zwiers, and M. D. Flannigan (2004), Detecting the effect of climate change on Canadian forest fires, *Geophys. Res. Lett.*, *31*, L18211, doi:10.1029/2004GL020876.

Goode, J. G., R. J. Yokelson, D. E. Ward, R. A. Susott, R. E. Babbitt, M. A. Davies, and W. M. Hao (2000), Measurements of excess O_3, CO_2, CO, CH_4, C_2H_4, C_2H_2, HCN, NO, NH_3, HCOOH, CH_3COOH, HCHO, and CH_3OH in 1997 Alaskan biomass burning plumes by airborne Fourier transform infrared spectroscopy (AFTIR), *J. Geophys. Res.*, *105*, 22,147–22,166.

Gupta, M. L., R. J. Cicerone, D. R. Blake, R. S. Rowland, and I. S. Isaksen (1998), Global atmospheric distributions and source strengths of light hydrocarbons and tetrachloroethene, *J. Geophys. Res.*, *103*, 28,219–28,235.

Holzinger, R., J. Williams, G. Salisbury, T. Klupfel, M. De Reus, M. Traub, and P. J. Crutzen (2005), Oxygenated compounds in aged biomass burning plumes over eastern Mediterranean: Evidence of strong secondary production of methanol and acetone, *Atmos. Chem. Phys.*, *5*, 39–46.

Hurst, D. F., D. W. T. Griffith, J. N. Carras, D. J. Williams, and P. J. Frasar (1994), Measurements of trace gases emitted by Australian savanna fires during the 1990 dry season, *J. Atmos. Chem.*, *18*, 33–56.

Irion, F. W., et al. (2002), The Atmospheric Trace Molecule Spectroscopy Experiment (ATMOS) version 3 data retrievals, *Appl. Opt.*, *41*, 6968–6979.

Isaev, A. P., G. N. Korovin, S. A. Bartalev, D. V. Ershov, A. Janetos, E. S. Kasischke, H. H. Shugart, N. H. F. French, B. E. Orlick, and T. L. Murphy (2002), Using remote sensing to assess Russian forest fire carbon emissions, *Clim. Change*, *55*, 235–249.

Jacob, D. J., B. D. Field, Q. Li, D. R. Blake, J. de Gouw, C. Warneke, A. Hansel, A. Wisthaler, H. B. Singh, and A. Guenther (2005), Global budget of methanol: Constraints from atmospheric observations, *J. Geophys. Res.*, *110*, D08303, doi:10.1029/2004JD005172.

Jaffe, D., I. Bertschi, L. Jaeglé, P. Novelli, J. S. Reid, H. Tanamoto, R. Vangarzan, and D. L. Westfal (2004), Long-range transport of Siberian biomass burning emissions and impact on surface ozone in western north America, *Geophys. Res. Lett.*, *31*, L16106, doi:10.1029/2004GL020093.

Kajii, T., et al. (2002), Boreal forest fires in Siberia in 1998: Estimation of area burned and emissions of pollutants by advanced very high resolution radiometer satellite data, *J. Geophys. Res.*, *107*(D24), 4745, doi:10.1029/2001JD001078.

Kanakidou, M., B. Bonsang, J. C. Le Roulley, G. Lambert, D. Martin, and G. Senneqier (1988), Marine sources of atmospheric acetylene, *Nature*, *333*, 51–52.

Kasischke, E. S., E. J. Hyer, P. C. Novelli, L. P. Bruhwiler, N. H. F. French, A. I. Sukhinin, J. H. Hewson, and B. J. Stocks (2005), Influences of boreal fire emissions on northern hemisphere atmospheric carbon and carbon monoxide, *Global Biogeochem. Cycles*, *19*, GB1012, doi:10.1029/2004GB002300.

Khahil, M. A. K. (Ed.) (2000), *Atmospheric Methane: Its Role in the Global Environment*, 351 pp., Springer, New York.

Kleinböhl, A., G. C. Toon, B. Sen, J.-F. Blavier, D. K. Weisenstein, and P. O. Wennberg (2005), Infrared measurements of atmospheric CH_3CN [2005], *Geophys. Res. Lett.*, *32*, L23807, doi:10.1029/2005GL024283.

Ko, M., N. D. Sze, W.-C. Wang, G. Shia, A. Goldman, F. J. Murcray, D. G. Murcray, and C. P. Rinsland (1993), Atmospheric sulfur hexafluoride: Sources, sinks, and greenhouse warming, *J. Geophys. Res.*, *98*, 10,499–10,507.

Koch, D., and J. Hansen (2005), Distant origins of Arctic black carbon: A Goddard Institute for Space Studies ModelE experiment, *J. Geophys. Res.*, *110*, D04204, doi:10.1029/2004JD005296.

Koppmann, R., K. von Czapiewski, and J. S. Reid (2005), A review of biomass burning emissions, part 1: Gaseous emissions of carbon monoxide, methane, volatile organic compounds, and nitrogen containing compounds, *Atmos. Chem. Phys. Discuss.*, *5*, 10,455–10,516.

Lewis, A. C., J. R. Hopkins, L. J. Carpenter, J. Stanton, K. A. Read, and M. J. Pilling (2005), Sources and sinks of acetone, methanol, and aldehyde in North Atlantic marine air, *Atmos. Chem. Phys.*, *5*, 1963–1974.

Li, Q., D. J. Jacob, I. Bey, R. M. Yantosca, Y. Zhao, Y. Kondo, and J. Notholt (2000), Atmospheric hydrogen cyanide (HCN): Biomass burning source, ocean sink?, *Geophys. Res. Lett.*, *27*, 357–360.

Liu, J., J. R. Drummond, Q. Li, J. C. Gille, and D. C. Ziskin (2005), Satellite mapping of CO emissions from forest fires in northwest America using MOPITT measurements, *Remote Sens. Environ.*, *95*, 502–516.

Logan, J. A., M. J. Prather, S. C. Wofsy, and M. B. McElroy (1981), Tropospheric chemistry: A global perspective, *J. Geophys. Res.*, *86*, 7210–7254.

Manabe, S., M. J. Spellman, and R. J. Stouffer (1992), Transient responses of a coupled ocean-atmosphere model to gradual changes in atmospheric CO_2, *J. Clim.*, *5*, 105–126, doi:10.1175/1520-0442.

Morris, G. A., et al. (2006), Alaskan and Canadian forest fires exacerbate ozone pollution over Houston, Texas, on 19 and 20 July 2004, *J. Geophys. Res.*, *111*, D24S03, doi:10.1029/2006JD007090.

Nance, J. D., P. V. Hobbs, L. F. Radke, and D. E. Ward (1993), Airborne measurements of gases and particles from an Alaskan wildfire, *J. Geophys. Res.*, *98*, 14,873–14,882.

Norton, R. H., and C. P. Rinsland (1991), ATMOS data processing and science analysis methods, *Appl. Opt.*, *30*, 389–400.

Notholt, J., et al. (2003), Enhanced upper topical tropospheric COS: Impact on the stratospheric aerosol layer, *Science*, *300*, 307–310.

Paton-Walsh, C., N. B. Jones, S. R. Wilson, V. Harverd, A. Meier, D. W. T. Griffith, and C. P. Rinsland (2005), Measurements of trace gas emissions from Australian forest fires and correlations with coincident measurements of aerosol optical depth, *J. Geophys. Res.*, *110*, D24305, doi:10.1029/2005JD006202.

Pfister, G., P. G. Hess, L. K. Emmons, J.-F. Lamarque, C. Wiedinmyer, D. P. Edwards, G. Pétron, J. C. Gille, and G. W. Sachse (2005), Quantifying CO emissions from the 2004 Alaskan wildfires using MOPITT CO data, *Geophys. Res. Lett.*, *32*, L11809, doi:10.1029/2005GL022995.

Rinke, A., K. Dethloff, and M. Fortmann (2004), Regional climate effects of Arctic haze, *Geophys. Res. Lett.*, *31*, L16202, doi:10.1029/2004GL020318.

Rinsland, C. P., et al. (1998), ATMOS/ATLAS 3 infrared profile measurements of trace gases in the November 1994 tropical and subtropical upper troposphere, *J. Quant. Spectrosc. Radiat. Transfer*, *60*, 891–901.

Rinsland, C. P., E. Mahieu, R. Zander, P. Demoulin, J. Forrer, and S. Reimann (2000), Free tropospheric CO, C_2H_6 and HCN above central Europe:

Recent measurements from the Jungfraujoch station including the detection of elevated columns during 1998, *J. Geophys. Res.*, *105*, 24,235–24,249.

Rinsland, C. P., A. Goldman, E. Mahieu, R. Zander, J. Notholt, N. B. Jones, D. W. T. Griffith, T. M. Stephen, and L. S. Chiou (2002), Ground-based infrared spectroscopic measurements of carbonyl sulfide: Tropospheric trends from a 24-year time series of solar absorption measurements, *J. Geophys. Res.*, *107*(D22), 4657, doi:10.1029/2002JD002522.

Rinsland, C. P., E. Mahieu, R. Zander, A. Goldman, S. Wood, and L. Chiou (2004), Free tropospheric measurements of formic acid (HCOOH) from infrared ground-based solar absorption spectra: Retrieval approach, evidence for a seasonal cycle, and comparison with model calculations, *J. Geophys. Res.*, *109*, D18308, doi:10.1029/2004JD004917.

Rinsland, C. P., G. Dufour, C. D. Boone, P. Bernath, and L. S. Chiou (2005a), Atmospheric chemistry experiment (ACE) measurements of elevated Southern Hemisphere upper tropospheric CO, C_2H_6, HCN, and C_2H_2 mixing ratios from biomass burning emissions and long-range transport, *Geophys. Res. Lett.*, *32*, L20803, doi:10.1029/2005GL024214.

Rinsland, C. P., D. C. Boone, K. A. Walker, and B. F. Bernath (2005b), Comparison of profiles retrieved from measurements by the Atmospheric Chemistry Experiment (ACE): Tropospheric and stratospheric species, paper presented at 60th International Symposium on Molecular Spectroscopy, Ohio State Univ., Columbus.

Rinsland, C. P., et al. (2006a), First space-based observations of formic acid (HCOOH): Atmospheric chemistry experiment Austral spring 2004 and 2005 Southern Hemisphere tropical-mid-latitude upper tropospheric measurements, *Geophys. Res. Lett.*, *33*, L23804, doi:10.1029/2006GL027128.

Rinsland, C. P., A. Goldman, J. W. Elkins, L. Chiou, J. W. Hannigan, S. W. Wood, E. Mahieu, and R. Zander (2006b), Long-term trend of CH_4 at northern mid-latitudes: Comparison between infrared solar and surface sampling measurements, *J. Quant. Spectrosc. Radiat. Transfer*, *97*, 457–466.

Rinsland, C. P., P. F. Coheur, H. Herbin, C. Clerbaux, C. Boone, P. Bernath, and L. S. Chiou (2007), Detection of elevated tropospheric H_2O_2 (hydrogen peroxide) mixing ratios in ACE (Atmospheric Chemistry Experiment) subtropical infrared solar occultation spectra, *J. Quant. Spectrosc. Radiat. Transfer*, in press.

Rothman, L. S., et al. (2005), The HITRAN 2004 molecular spectroscopy database, *J. Quant. Spectrosc. Radiat. Transfer*, *96*, 139–204.

SAGE III ATBD Team (2002), SAGE III Algorithm Theoretical Basis Document (ATBD) Transmission Level 1B products (2002), Version 2.1, *LaRC 475-00-108*, NASA Langley Res. Center, Hampton, Va.

Schade, G. W., and A. H. Goldstein (2006), Seasonal measurements of acetone and methanol: Abundances and implications for atmospheric budgets, *Global Biogeochem. Cycles*, *20*, GB1011, doi:10.1029/2005GB002566.

Seiler, W., and P. J. Crutzen (1980), Estimates of gross and net fluxes of carbon between the biosphere and the atmosphere from biomass burning, *Clim. Change*, *2*, 207–247.

Shirai, T., et al. (2003), Emission estimates of selected volatile organic compounds from tropical savannah burning in Northern Australia, *J. Geophys. Res.*, *108*(D3), 8406, doi:10.1029/2001JD000841.

Singh, H. B., Y. Chen, A. Staudt, D. Jacob, D. Blake, B. Heikes, and J. Snow (2001), Evidence from the Pacific troposphere of large global sources of oxygenated organic compounds, *Nature*, *410*, 1078–1081.

Singh, H. B., et al. (2003), In situ measurements of HCN and CH_3CN over the Pacific Ocean: Sources, sinks, and budgets, *J. Geophys. Res.*, *108*(D20), 8795, doi:10.1029/2002JD003006.

Singh, H. B., et al. (2004), Analysis of the atmospheric distribution, sources, and sinks of oxygenated volatile organic chemicals based on measurements over the Pacific during TRACE-P, *J. Geophys. Res.*, *109*, D15S07, doi:10.1029/2003JD003883.

Smyth, S., et al. (1999), Characterization of the chemical signatures of air masses observed during the PEM experiments over the western Pacific, *J. Geophys. Res.*, *104*, 16,243–16,254.

Stocks, B. J., M. A. Fosberg, and T. J. Lynham (1998), Climate and forest fire potential in Russia and Canadian boreal forests, *Clim. Change*, *38*, 1–13.

Tans, P., P. P. S. Bakwin, and D. W. Guenther (1996), A feasible global carbon cycle observing system: A plan to decipher today's carbon cycle based on observations, *Global Change Biol.*, *2*, 309–318.

Thomason, L. W., and T. Taha (2003), SAGE III aerosol extinction measurements: Initial results, *Geophys. Res. Lett.*, *30*(12), 1631, doi:10.1029/2003GL017317.

Turquety, S., et al. (2007), Inventory of boreal fire emissions for North America in 2004: Importance of peat burning and pyroconvective injection, *J. Geophys. Res.*, *112*, D12S03, doi:10.1029/2006JD007281.

Vander Awera, J. W., and K. Didriche (2004), Absolute intensities in the ν_6 band of trans-formic acid, paper RB11, paper presented at 59th Ohio State University Symposium on Molecular Spectroscopy, Univ. of Ohio, Columbus.

Wang, P.-H. (1994), SAGE II tropospheric measurement frequency and its meteorological implication, paper presented at Seventh Conference on Satellite Meteorology and Oceanography, Am. Meteorol. Soc., Boston, Mass.

Wang, P.-H. (1996), A 6-year climatology of cloud occurrence frequency from stratospheric aerosol and gas experiment II observations (1985–1990), *J. Geophys. Res.*, *101*, 29,407–29,429.

World Meteorological Organization (2006), Controlled substances and other source gases, in *Scientific Assessment of Ozone Depletion: 2006*, *Global Ozone Res. Monit. Proj. Rep.* 50, pp. 1.1–1.83, Global Ozone Res. and Monit. Proj., Geneva.

Wotton, B. M., and M. D. Flannigan (1993), Length of the fire season in a changing climate, *For. Chron.*, *69*, 187–192.

Yokelson, R. J., R. Susott, D. E. Ward, J. Reardon, and D. W. T. Griffith (1997), Emissions from smoldering combustion of biomass measured by open-path Fourier transform infrared spectroscopy, *J. Geophys. Res.*, *102*, 18,865–18,877.

Yokelson, R. J., J. G. Goode, D. E. Ward, J. A. Susott, R. E. Babbit, D. D. Wade, I. Bertschi, D. W. T. Griffith, and W. M. Hao (1999), Emissions of formaldehyde, acetic acid, methanol, and other trace gases from biomass fires measured by airborne Fourier transform infrared spectroscopy, *J. Geophys. Res.*, *104*, 30,109–30,125.

Yokelson, R. L., I. T. Bertschi, T. J. Christian, P. V. Hobbs, D. E. Ward, and W. M. Hao (2003), Trace gas measurements in nascent, aged, and cloud-processed smoke from African savanna fires by airborne Fourier transform infrared spectroscopy (AFTIR), *J. Geophys. Res.*, *108*(D13), 8478, doi:10.1029/2002JD002322.

Yoshida, Y., Y. Wang, T. Zeug, and R. Yantosca (2004), A three-dimensional global model study of atmospheric methyl chloride budget and distributions, *J. Geophys. Res.*, *109*, D24309, doi:10.1029/2004JD004951.

Yurganov, L. N., et al. (2004), A quantitative assessment of the 1998 carbon monoxide emission anomaly in the Northern Hemisphere based on total column and surface concentration measurements, *J. Geophys. Res.*, *109*, D15305, doi:10.1029/2004JD004559.

Zhao, Y., et al. (2002), Spectroscopic measurements of tropospheric CO, C_2H_6, C_2H_2, and HCN in northern Japan, *J. Geophys. Res.*, *107*(D18), 4343, doi:10.1029/2001JD000748.

P. F. Bernath, Department of Chemistry, University of York, York Y010 5DD, UK. (pfb500@york.ac.uk)

C. D. Boone, Department of Chemistry, University of Waterloo, Waterloo, Ontario, Canada N2L 3G1. (cboone@acebox.uwaterloo.ca)

L. Chiou, Science Systems and Applications, Inc., 1 Enterprise Parkway, Suite 200, Mail Stop 927, Hampton, VA 23666, USA. (l.s.chiou@larc.nasa.gov)

P.-F. Coheur, Chimie Quantique et Photophysique, Université Libre de Bruxelles, 50, Avenue F.D. Roosevelt, Brussels B-1050, Belgium. (pfcoheur@ulb.ac.be)

C. Clerbaux and S. Turquety, Service d'Aéronomie/Institut Pierre-Simon Laplace, Université Pierre et Marie Curie-Paris 6, 4, Place Jussieu, Cedex 05, Paris F-75252, France. (ccl@aero.jussieu.fr; stu@aero.jussieu.fr)

G. Dufour, Laboratoire de Météorologie Dynamique/Institut Pierre-Simon Laplace, Route départementale 36, Palaiseau F-91128, France. (gaelle.dufour@lmd.polytechnique.fr)

C. P. Rinsland, NASA Langley Research Center, Mail Stop 401A, Hampton, VA 23681-2199, USA.